Sulfonated Reduced Graphene Oxide: An Acid Catalyst that Efficiently Promotes the Esterification of Glycerol

Luisa Damaris Ramos Riascos, Alfonso Enrique Ramírez Sanabria, Gerardo Andrés Torres Rodríguez, Alexander Sachse, Cristian David Miranda Muñoz

Sulfonated Reduced Graphene Oxide: An Acid Catalyst that Efficiently Promotes the Esterification of Glycerol

Luisa Damaris Ramos Riascos[1] · Alfonso Enrique Ramírez Sanabria[1] · Gerardo Andrés Torres Rodríguez[2] · Alexander Sachse[3] · Cristian David Miranda Muñoz[1]

Abstract

A sulfonated graphene catalyst was designed and tested in the acetylation of glycerol. The catalyst was synthesized using graphite as starting material and comprised three stages, which included: (i) synthesis the graphene oxide by means of a modified Hummers method, (ii) reduction with ascorbic acid, and (iii) functionalization of the material with sulfanilic acid by in situ diazotization. Structural, morphological and chemical properties were characterized by SEM, XRD, and FT-IR spectroscopy. The acidity was determined by elemental analysis. The catalytic properties of catalyst in the glycerol acetylation were studied and compared with a commercial sulfonic resin, i.e. Amberlyst® 15. The sulfonated graphene presents attractive features in the catalytic transformation of glycerol, allowing for significant increase in the reaction rate at low temperature, and achieving at optimum activity and greater selectivity towards triacetin.

Keywords Reduced sulfonated graphene oxide · Heterogeneous catalysis · Glycerol acetylation · Glycerol valorization

1 Introduction

The booming production of biodiesel has brought an overproduction of glycerol, as unavoidable synthetic by-product, which corresponds to approximately 10% of the products in weight [1]. A consequence of this is the quest of sound glycerol valorization strategies [2]. An attractive possibility is the chemical transformation of glycerol towards oxygenated biofuel additives. This would be advantageous for the biodiesel industry through favoring the establishment of a circular, profitable and sustainable industry [3].

In this context, the glycerol acetylation is considered as an excellent alternative to obtain oxygenated biofuel additives [4], as mono-, di- and triacetyled glycerol (MAG + DAG + TGA) can be obtained [5]. Specifically, triacetin (TGA) is promising as fuel additive [6], allowing to improve the cold flow properties of conventional diesel fuel, increasing the cetane number and reducing the emission of harmful gases [7]. However, triacetin is the most unfavored product using acetic acid as a reagent. Its production requires hence the use of a catalyst [8].

Glycerol acetylation is traditionally promoted by homogeneous acid catalysts such as sulfuric acid (H_2SO_4), phosphoric acid (H_3PO_4) and hydrochloric acid (HCl). Nevertheless, homogeneous acid catalysts present important issues related to the production of toxic compounds, reactor corrosion and product separation [9]. Hence their replacement with heterogeneous catalysts is sought. Acid catalysis is widely used in the chemical industry as a large variety of chemical transformations requires the involvement of acids [10]. For instance, acidic resins (e.g. Amberlyst® 15) [11], zeolites [12] clays [13], functionalized metal oxides [14] and sulfonic acid-functionalized carbons [15] are some examples of frequently employed aid catalyst that allow for achieving superior performances [16].

Graphene related materials are an emerging class of promising heterogeneous catalytic systems, due to their 2D structure, high stability and flexibility of functionalization [17]. These often feature defined textures with uniform pore

✉ Cristian David Miranda Muñoz
cdmiranda@unicauca.edu.co

[1] Grupo de Catálisis, Departamento de Química, Universidad del Cauca, calle 5 No. 4-70, Popayán, Colombia

[2] Grupo de Microscopía y Análisis de Imágenes, Departamento de Biología, Universidad del Cauca, calle 5 No. 4-70, Popayán, Colombia

[3] Institut de Chimie des Milieux et Matériaux de Poitiers (ICM2P), UMR 7285 CNRS, 4 Rue Michel Brunet, Bâtiment B27, 86073 Poitiers Cedex, France

sizes, among other properties, that positively influence their adsorption behavior and their catalytic properties. As an example, sulfonated graphene oxide, obtained by functionalization of GO with $–SO_3H$ groups, proved as excellent solid acid catalyst in organic transformations [17–19], featuring waterproof properties [20] and considerable thermal stability [21]. Recently some of us reported improved glycerol etherification using sulfonated graphene oxide and allowed for the superior production of poly-substituted ethers [22].

In the present work, we firstly report the use of sulfonated graphene oxide in the glycerol acetylation. The results prove for a very active, selective and stable catalyst under the chosen reactions conditions.

2 Experimental

2.1 Materials

Glycerol ($C_3H_8O_3$, 99%, Fisher), acetic acid ($C_2H_4O_2$, 99.7% EM Science), Amberlyst® 15 (Dry, Across Organic), graphite powder (< 20 µm, synthetic, Sigma-Aldrich), sulfuric acid (H_2SO_4, 95–97%, Merck), potassium permanganate ($KMnO_4$, Mallinckrodt, AR 99%), hydrogen peroxide (H_2O_2, 30%, AppliChem Panreac), ethyl acetate ($C_4H_8O_2$, 99.9%, Fisher Scientific), methanol (CH_3OH, ≥ 99.9%, Emsure®), sodium nitrite ($NaNO_3$, 99%, Merck), sulfanilic acid ($C_6H_7NO_3S$, 99.3%, Fisher Chemicals), acetone (C_3H_6O, 99.9%, Mallinckrodt AR), hydrochloric acid (HCl, 37%, Fisher Scientific) and ascorbic acid (commercial, C_6H_8O) were used as received.

2.2 Sulfonated Graphene Synthesis

2.2.1 Graphene Oxide (GO) Synthesis

Graphene oxide (GO) was obtained by a modification of the Hummer's method [22]. For the modified method, H_2SO_4 (55 mL) was added to a mixture of graphite powder (2.1 g) and $KMnO_4$ (7.5 g) in an ice bath. The reaction was then heated to 35 °C and stirred for 2 h. 30% H_2O_2 (6 mL) was diluted with in deionized water (80 mL) and poured onto ice (≈ 5 °C). Then, deionized water (150 mL) was added and stirred all night long at rt. For workup, the mixture was centrifuged (5000 rpm for 10 min), and the supernatant was decanted and the solid was dried at 60 °C during 24 h.

2.2.2 Graphene Oxide (GO) Reduction [(GO)R]

Graphene oxide (0.513 g) was added to deionized water (600 mL) and stirred to form a suspension. The suspension was sonicated 2 h and then ascorbic acid (164.1 g) was added and stirred for 2 h at 80 °C. The reaction was cooled to rt and then filtered through a nylon filter (Whatman 0.45 µm, 47 mm). The filtrate was then washed with 25 mL of deionized water, 40 mL of methanol and 40 mL of ethyl acetate (4×) [22]. The solid (GO)R was then dried to 60 °C by 12 h.

2.2.3 Reduced Graphene Oxide [(GO)R] sulfonation [(GO)RS]

Sulfonation of (GO)R was carried out by in situ diazotization with sulfanilic acid. (GO)R (0.276 g) was added to deionized water (40 mL) and sonicated 2 h. A mixture of $NaNO_3$ (0.95 g) and $C_6H_7NO_3S$ (0.795 g) was incorporated. The reaction was stirred at 25 °C for 24 h. The solid was filtered through a nylon filter (Whatman 0.45 µm, 47 mm). The filtrate was then washed with 50 mL of 1.0 M HCl and 70 mL of acetone (3×) [22]. The solid (GO)RS was then dried to 50 °C by 12 h.

2.3 Characterization Techniques

X-ray diffraction (XRD) analysis was performed using a Xpert PANalytical Empyrean Series II-Alpha 1with a Cu–K_α as radiation source. The measurements were performed with step size of 0.05 and a scan rate of 1° min^{-1} from 20 to 60° 2θ.

Sulfonic groups in surface were detected by FT-IR (Fourier transform infrared spectroscopy) in Attenuated Total Reflection (ATR) using a spectrophotometer Nicolet™ iS™.

Structural, morphological and textural properties were investigated by scanning electron microscopy (SEM). The images were obtained by using a microscope Zeiss EVO HD15. Samples were dispersed as a powder onto copper grids coated with carbon film.

Acidity was assessed by elemental analysis and calculated as reported by Oger [18] using a CHNS elemental analyzer vario EL cube.

2.4 Catalyst Testing

The reaction was carried out in a glass autoclave reactor, provided with temperature control, a manometer and stirring control. For the acetylation studies molar ratios of 1:3, 1:6 and 1:9 glycerol:acetic acid were studied and a constant catalyst loading of 5% (with respect to the glycerol mass) was used in all experiments. The total reaction volume was adjusted to 14 mL. 0.3 mL of sample was taken directly from the reaction and subjected to centrifugation. The reaction was followed at 8, 17, 25, 33, 42, 50, 60, 90 and 120 min. Additionally, a set of temperatures was evaluated (70, 90 and 110 °C) under constant and continuous stirring (1100 rpm). Amberlyst® 15 (A15) was used as reference catalyst.

2.5 Analysis of Products

The qualitative analysis was performed by Gas Chromatography coupled to Mass Spectroscopy (GC–MS) using a chromatograph Thermo Scientific model Trace 1300, HP-5MS column (30 m, 0.25 mm, 0.25 µm), a MS model ISQL detector and ethylene glycol (99%, Sigma Aldrich) as internal standard. The quantitative analysis was performed by Gas Chromatography using a chromatograph model Shimadzu GC-14A, DB-WAX column (30 m, 0.25 mm, 0.25 µm), an FID detector and ethylene glycol (99%, Sigma Aldrich) as internal standard. The temperature program used consisted of an isotherm at 100 °C (1 min), an increase rate of 20 °C/min until reaching 240 °C, where there was another isotherm for 2 min. The samples for injection (0.1 µL) for analysis were prepared as a mixture (200 mg of sample and 20 mg of internal standard). The response factors of products (mono-, di- and triacetin) were determined by calibration performed with standards.

2.6 Catalytic Properties

2.6.1 Activity

Catalytic activity was determined from the glycerol conversion

$$\text{Glycerol conversion}\,(\%) = \frac{\text{Moles of reacted glycerol}}{\text{Moles of initial glycerol}} \times 100$$

$$\text{Activity} = \frac{\text{moles of reacted glycerol}}{\text{Time (h)} \times \text{mmol } H^{+}}$$

The molar yield was also calculated

$$\text{Molar yield}\,(\%) = \frac{\text{Moles of obtained product}}{\text{Moles of initial glycerol}} \times 100$$

2.6.2 Triacetin Selectivity

The response factors of products (mono-, di- and triacetin) were used to evaluate the selectivity.

$$\text{Triacetin selectivity}\,(\%) = \frac{\text{Moles of obtained triacetin}}{\text{Total moles of products}}$$

2.6.3 Recyclability

After each catalytic cycle, the catalyst was separated by centrifugation using a centrifuge (Hermle Z206A), washed with deionized water and ethanol (Sigma-Aldrich, 96%) and was then dried at 60 °C for 20 h.

3 Results and Discussion

3.1 Characterization of Solids

3.1.1 X-ray Diffraction (XRD)

To verify that the used synthesis process allowed for the formation of the desired solids, the XRD patterns were recorded (Fig. 1). For the starting material, graphite, the XRD pattern shows a characteristic peak at 26.5° 2θ, corresponding to the (002) reflection, while the XRD pattern of GO shows a main diffraction peak of approximately 11.2° 2θ, attributed to the (001) diffraction plane. The absence of the (002) reflection in the GO sample indicates that the graphite oxidation was complete [23]. Using Bragg's law, the interplanar spacing was calculated, which amounts to 0.80 and 0.34 nm for GO and graphite, respectively. The increase in the d-spacing upon oxidation is due to the insertion of oxygenated functional groups generating electronic repulsion and therefore higher spacing between layers [24], as well as a greater affinity for water molecules [25], which was further corroborated by FT-IR spectroscopy (Fig. 2). For GO, a broad peak at approximately 2θ = 42.3° was observed, which can be ascribed to the (100) plane [26]. Indeed, Diffraction peaks in GO are due to the short-range order of stacked graphene layers [27]. After reduction of GO with ascorbic acid [(GO)R], the oxygen-containing functional groups are removed, resulting in a shift of the 001 reflection to 25.3° 2θ, indicating a reduction of the interplanar spacing to 0.36 nm and a faint band at 43.4° 2θ (100). The enlargement of the diffraction peaks suggest a degradation of the long range structural order during the exfoliation step [18]. Finally, the sulfonation treatment has little impact on

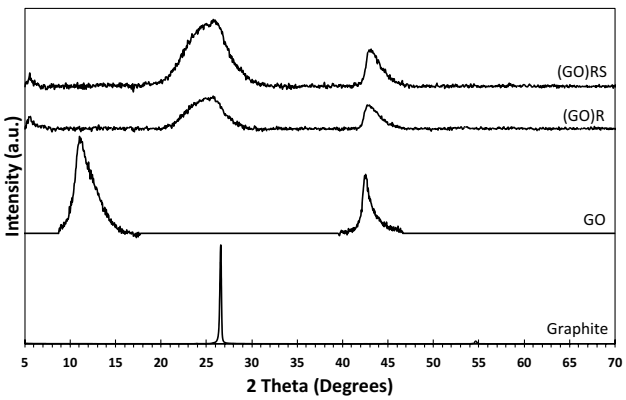

Fig. 1 X-ray diffraction of graphite, GO, (GO)R and (GO)RS

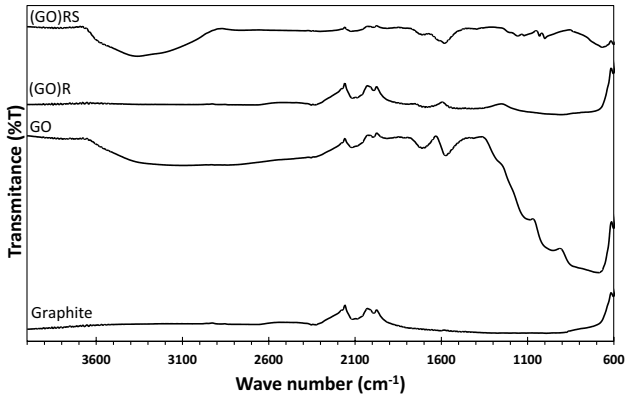

Fig. 2 FT-IR spectra of graphite, GO, (GO)R and (GO)RS

the structural properties, as the XRD pattern of (GO)RS resembles the one of (GO)R.

3.1.2 Fourier Transform Infrared Spectroscopy (FT-IR)

The FT-IR spectra (Fig. 2), allow to observe the structural changes in the materials from graphite to (GO)RS. GO exhibits a broad band at approximately 3115 cm^{-1}, corresponding to the stretching vibrations of the –OH bonds of the carboxyl groups (–COOH) and to the water molecules absorbed in the material. A band at 1711 cm^{-1}, associated with the vibrations of the carbonyl group (C=O) and a band at 851 cm^{-1}, related to the epoxide bonds (C–O–C) [28], can be further observed. Characteristic bands of the asymmetric and symmetric O=S=O stretching vibrations were also observed at 1115 cm^{-1} and 998 cm^{-1}, which were attributed to remnants of sulfuric acid product of the GO synthesis [29]. The reduction of GO was verified by the disappearance of both the bands associated with the oxygenated groups and the signals corresponding to the sulfate group in the (GO)R spectrum. Finally, the (GO)RS exhibits characteristic bands associated with the sulfonic group at 1103 cm^{-1} and 996 cm^{-1}, indicating successful surface grafting. In addition, the presence of a broad band at 2926 cm^{-1} indicates an increase in the polarity of the material with respect to the original material (GO)R, related to the insertion of the sulfonic group and the gain in Brønsted acidity.

3.1.3 Scanning Electron Microscopy (SEM)

Scanning electron microscopy has been used to investigate the evolution of the morphology of the materials after each synthesis step. Figure 3 shows the SEM images of graphite, GO, (GO)R and (GO)RS. For graphite dispersed particles with rather uniform granular size and shape can be observed. The GO, (GO)R and (GO)RS materials are heterogeneous in both size and shape forming smaller clusters with porous structure. The surfaces of graphene sheets are not perfectly flat presenting surface wrinkles as previously reported by Chen et al., which is related to different levels of transparency [30].

3.1.4 Acidity Calculated by Elemental Analysis

The results of the elemental analysis are shown in Table 1. The sulfur content may be associated with the presence of sulfate groups or it may be related to the grafting of $–SO_3H$ groups.

Initially, the presence of remaining sulfate groups in the GO, associated with the use of sulfuric acid in the synthesis, is detected. The reduction process allows these groups to be removed from the surface and subsequently only sulfonic groups are grafted, which provide the Brønsted acidity in the catalyst.

3.2 Catalytic Evaluation

Acetylation of glycerol with acetic acid is illustrated in Scheme 1. The mono-, di- and tri-acetylated products MAG (two isomers), DAG (two isomers) and TAG are formed as well as water as a byproduct. The reversible character of the reaction allows for the evaluation of different parameters on the chemical equilibrium [31].

To examine the parameters that influence the reaction, Amberlyst® 15 was used as the reference catalyst and the optimal conditions of temperature, glycerol/acetic acid molar ratio and reaction time were evaluated as a function of glycerol conversion. The suitable amount of catalyst was determined to be 5% by mass with respect to the total mass amount of glycerol. The stirring speed was set to 1100 rpm, where external mass transfer limitations are negligible [32].

3.2.1 Effect of Reaction Temperature

The effect of temperature was evaluated at 70, 90 and 110 °C, using a 1:9 molar ratio of glycerol:acetic acid, during two hours of reaction. The results shown in Fig. 4 suggest a temperature dependency of the glycerol acetylation reaction. The maximum conversion was obtained at 110 °C, which can be attributed to the faster formation of acylium ions with increasing temperature [33]. Furthermore, an increase in the reaction temperature favors collision of reactant molecules, increasing the reaction rate. As far as selectivity is concerned, a proportional increase of TAG selectivity with temperature was observed. According to Scheme 1, a successive transformation of MAG → DAG → TAG occurs, which is favored when equilibrium is reached, it is hence possible to produce more TAG, when increasing temperature of 110 °C. Hence, reaction temperature was set to 110 °C in further tests.

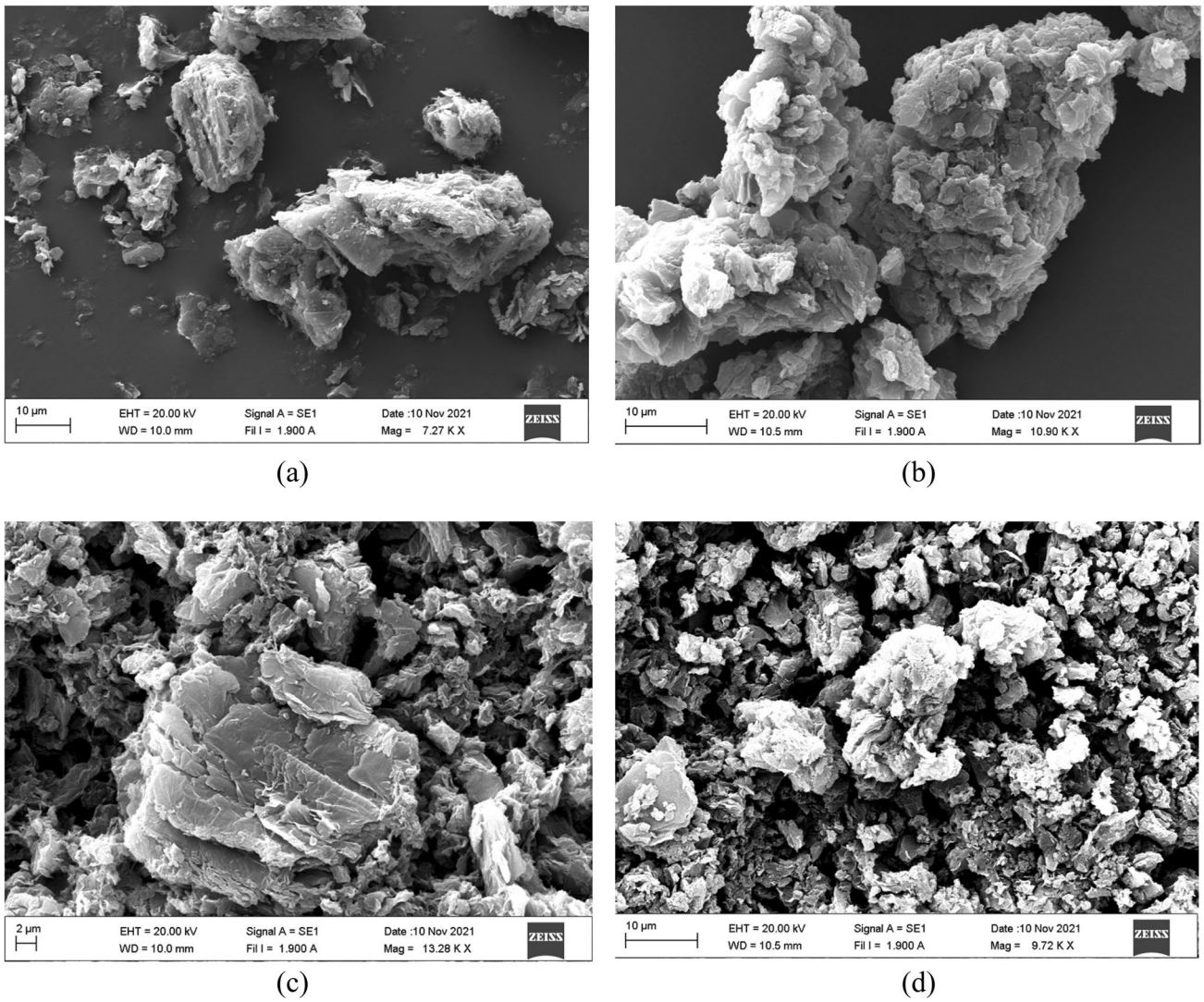

Fig. 3 SEM images of **a** graphite, **b** GO, **c** (GO)R and **d** (GO)RS

Table 1 Elemental analysis for (GO)R and (GO)RS in comparison to Amberlyst® 15

Material	Elemental analysis (%)				Acidity (mmol H^+ g^{-1})
	C	H	N	S	
A-15	–	–	–	–	2.37*
GO	21.36 + 1.01	1.45 + 0.50	–	11.00 + 0.29	3.43**
(GO)R	78.74 + 0.03	0.88 + 0.01	0.02 + 0.00	0.11 + 0.01	0.03**
(GO)RS	64.93 + 0.07	1.90 + 0.02	0.11 + 0.01	5.37 + 0.01	1.68***

*Measured by Pyr-IR adsorption [22]

**Remaining sulfate groups

***Associated with $–SO_3H$ groups

3.2.2 Effect of Glycerol/Acetic Acid Molar Ratio

The influence of the glycerol/acetic acid molar ratio was studied by setting the ratios to 1:3, 1:6 and 1:9. The temperature was adjusted to 110 °C, 5% catalyst loading (Amberlyst® 15), and the reaction was held for 2 h. A higher glycerol conversion and TAG yield can be observed with increasing glycerol/acetic acid molar ratio (Fig. 5). This is due to the increase in the amount of acetic acid molecules in the reaction medium and therefore provides more acetylating

Scheme 1 Glycerol esterification with acid acetic

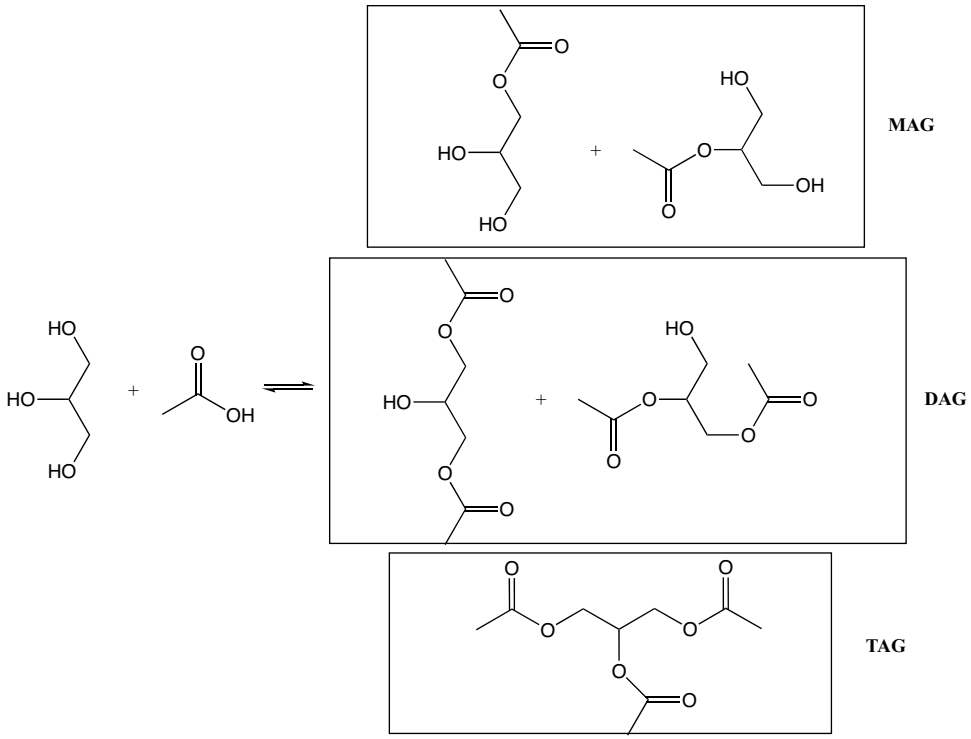

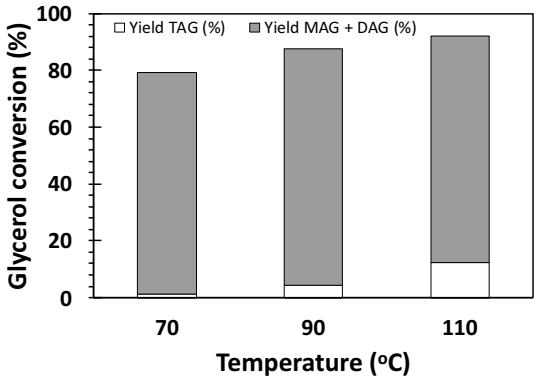

Fig. 4 Effect of reaction temperature. Reaction time = 2 h, glycerol:acetic acid molar ratio = 1:9, Catalyst loading: 5% by weight (relative to the mass of glycerol), stirring: 1100 rpm

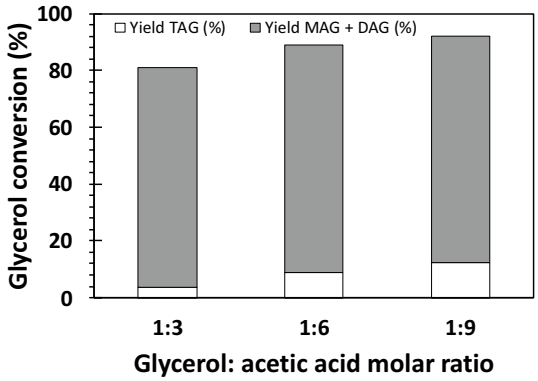

Fig. 5 Effect of glycerol:acetic acid molar ratio. Reaction time = 2 h, Temperature = 110 °C, Catalyst loading: 5% by weight (relative to the mass of glycerol), stirring: 1100 rpm

agent, hence facilitating the change in the distribution of esters towards more substituted species [32]. This correlates with what was reported by Khayoon et al. [15]. Finally, a molar ratio of 1:9 of glycerol/acetic acid was chosen as most suitable for the glycerol acetylation.

3.2.3 Effect of Reaction Time

The effect of reaction time on glycerol acetylation was studied using a glycerol/acetic acid ratio of 1:9, 110 °C, a catalyst loading of 5% (relative to the mass of glycerol) and stirring of 1100 rpm. Figure 6 shows the behavior of glycerol conversion and TAG selectivity during 7 h. As far as the conversion is concerned, a plateau is reached after two hours of reaction at 92%. For the selectivity a continuous formation of TAG is observed before reaching a plateau after 4 h at 26%. Indeed, glycerol acetylation follows a consecutive reaction mechanism, where TAG is formed by successive esterification of DAG present in the reaction medium [32].

3.2.4 Catalytic Properties

3.2.4.1 Catalytic Activity After establishing the conditions under which maximal glycerol was observed using A15 as

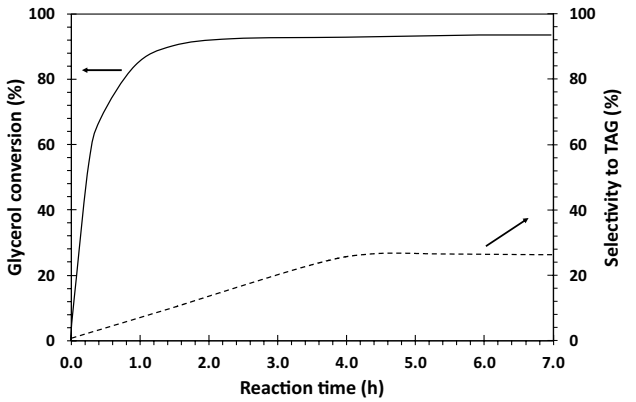

Fig. 6 Effect of reaction time. Temperature = 110 °C, glycerol:acetic acid molar ratio = 1:9, Catalyst loading: 5% by weight (relative to the mass of glycerol), stirring: 1100 rpm

a catalyst, the catalytic behavior of the (GO)RS solid was evaluated and compared to the one of GO (Fig. 7). A blank experiment (without catalyst) allowed to observe a conversion of 50% after 2 h, suggesting an autocatalytic effect promoted by the excess of acetic acid, which provides a Brønsted-type acidity to the medium and to the elevated reaction temperature (110 °C), which could favor glycerol conversion (endothermic reaction) [34].

Subsequently, a test using GO as catalyst was carried out, for which high catalytic activity was observed. The elemental analysis (Table 1), allows to deduce the presence of sulfur in the sample (residues from synthesis with sulfuric acid). These groups can leach into the reaction medium, generating a homogeneous process. This was verified by removing the GO catalyst from the reaction medium 5 min after the start of the reaction; Here for a similar conversion (~92%) was observed after 2 h as in the presence of the GO catalyst. In order to elaborate a truly heterogeneous catalyst GO

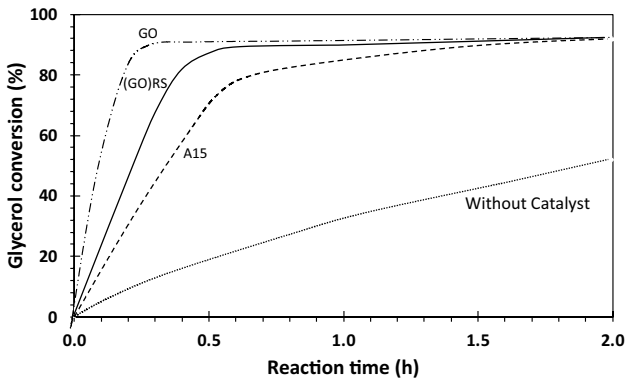

Fig. 7 Glycerol conversion (%) without catalyst and using A15, GO and (GO)RS catalysts. Temperature = 110 °C, glycerol: acetic acid molar ratio = 1:9, stirring: 1100 rpm

reduction process is required, which eliminates the sulfate groups (Table 1). Successive grafting of the sulfonic groups by diazotization then allows for the design of the heterogeneous acid catalyst.

The glycerol conversion obtained with the (GO)RS catalyst was the same as with A15 after two hours of reaction (92%). Yet a strong difference in the reaction rate and activity were observed. Both are significantly higher for the (GO)RS catalyst compared to A15 (Table 2).

These activity results indicate a buffer-like effect of the surface of the solid (GO)RS against the by-product water. Hence, despite A15 featuring a higher number of acidic sites (2.37 mmol H^+ g^{-1}) compared to (GO)RS (1.68 mmol H^+ g^{-1}), the oxygenated groups in the latter play a crucial role. (GO)RS presents approximately 20% of oxygen groups that can adsorb water formed during the reaction, hence the acid sites only little interact with H_2O molecules. Indeed, about 38 mmol of water is formed at 92% glycerol conversion. Several reports in the literature present strong adsorption of highly polar molecules, such as water, on resin surface [35, 36], which was not the case for sulfonated graphene oxide, for which catalytic activity was observed even in the presence of high amounts of water [20].

In addition, ln(Co/C) vs. reaction time was plotted to examine the reaction rate dependence. In Fig. S1 a linear relationship between the glycerol consumption and time can be observe for both A-15 and (GO)RS. These results suggest that under the applied conditions, i.e. a glycerol/acetic acid molar ratio of 1:9, 5% catalyst loading and 110 °C, a first order reaction occurs. These results are consistent with those observed in the same reaction promoted by heterogenized tungstophosphoric acid catalysts [37].

3.2.4.2 Selectivity Selectivity towards TAG with respect to glycerol conversion is shown in Fig. 8. Glycerol acetylation consists of a consecutive MAG → DAG → TAG transformation (Scheme 1), which, according to the obtained results, is favored when the maximum glycerol conversion is reached. When the glycerol conversion is highest, i.e. between 90 and 92%, a increased selectivity of TAG is observed for all catalysts. At isoconversion of glycerol (91.7%) A TAG selectivity of 25.0%, 19.6% and 13.5% is respectively observed using GO, (GO)RS and Amberlyst®15. As far as GO is

Table 2 Activity and reaction rate for A15 and (GO)RS

Catalyst	Rate (mol of glycerol reacted h^{-1})	Activity (mol of glycerol reacted h^{-1} mmol $H+^{-1}$)
A-15	50.3	170
(GO)RS	82.4	394

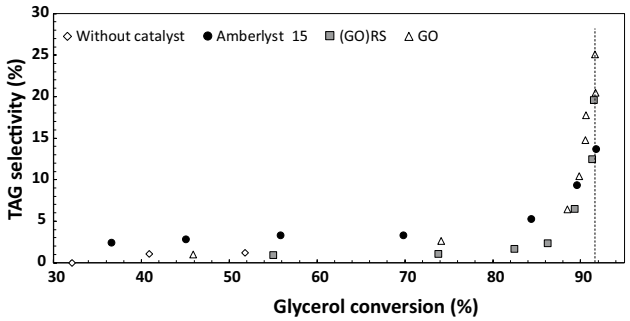

Fig. 8 TAG Selectivity vs. glycerol conversion using GO, (GO)RS and A15 as catalysts. Catalyst loading: 5% by weight (relative to the mass of glycerol), temperature = 110 °C, glycerol:acetic acid molar ratio = 1:9, stirring: 1100 rpm

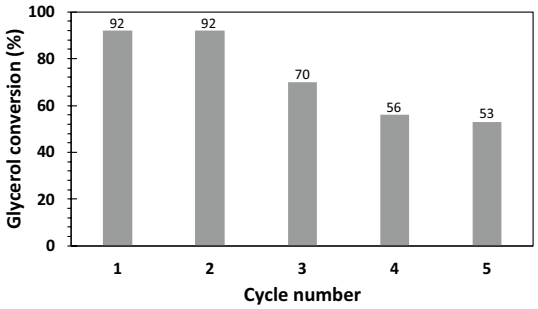

Fig. 9 (GO)RS catalyst stability study (5 reaction cycles). Catalyst loading: 5% by weight (relative to the mass of glycerol), temperature = 110 °C, glycerol:acetic acid molar ratio = 1:9, stirring: 1100 rpm

concerned, we previously discussed that the process corresponds rather to a homogeneous process in which sulfate groups are leached in the reaction medium. With respect to (GO)RS, it reaches equilibrium before A15, thus favoring the successive transformation of the products.

3.2.4.3 Stability The stability of the catalyst was evaluated by 5 recycling cycles (Fig. 9). The conversion of glycerol reduces slightly after the third reaction cycle and falls to ~ 55% after the fifth cycle.

The reduction in conversion upon recycling can be explained by the loss of -SO_3H groups, leading to a lower acidity of the recycled catalyst (Table 3). Indeed, water, which develops as unavoidable byproduct of the reaction, leads to the hydrolysis of the -SO_3H groups on the catalyst surface, hence reducing acidity [38].

4 Conclusion

A heterogeneous acid catalyst was successfully synthesized by sulfonation of reduced graphene oxide, allowing to graft –SO_3H groups onto the GO surface with an acidity of 1.68 mmol g^{-1}. The grafting of –SO_3H groups leads to significant catalytic activity in the glycerol acetylation compared to the commercial acid catalyst Amberlyst® 15. Interestingly it was found that the oxygenated groups in (GO)RS act as water scavengers, which allows for maintaining high catalyst activity, as water is an unavoidable by product of the glycerol acetylation. (GO)RS allowed for achieving superior selectivity towards the trisubstituted ester, which is the most desired product of the reaction. Slight reduction of catalytic activity of the (GO)RS in recycling experiments could be related to partial hydrolysis of the –SO_3H groups.

Supplementary Information The online version contains supplementary material available at https://doi.org/10.1007/s11244-022-01629-y.

Acknowledgements Authors express our acknowledges for the financial support obtained from VRI-UNICAUCA (Project ID 5526). A.S. acknowledges financial support from the European Union (ERDF) and "Région Nouvelle Aquitaine".

References

1. Okoye PU, Abdullah AZ, Hameed BH (2017) Synthesis of oxygenated fuel additives via glycerol esterification with acetic acid over bio-derived carbon catalyst. Fuel 209:538–544. https://doi.org/10.1016/j.fuel.2017.08.024
2. Pagliaro M, Ciriminna R, Kimura H et al (2007) From glycerol to value-added products. Angew Chemie Int Ed 46:4434–4440. https://doi.org/10.1002/anie.200604694
3. Reddy PS, Sudarsanam P, Raju G, Reddy BM (2010) Synthesis of bio-additives: acetylation of glycerol over zirconia-based solid acid catalysts. Catal Commun 11:1224–1228. https://doi.org/10.1016/j.catcom.2010.07.006
4. Gonçalves VLC, Pinto BP, Silva JC, Mota CJA (2008) Acetylation of glycerol catalyzed by different solid acids. Catal Today 133–135:673–677. https://doi.org/10.1016/j.cattod.2007.12.037
5. Aghbashlo M, Tabatabaei M, Rastegari H, Ghaziaskar HS (2018) Exergy-based sustainability analysis of acetins synthesis through continuous esterification of glycerol in acetic acid using Amberlyst®36 as catalyst. J Clean Prod 183:1265–1275. https://doi.org/10.1016/j.jclepro.2018.02.218

Table 3 Elemental analysis for (GO)RS in comparison to (GO)RS-reused (5th cycle)

Material	Elemental analysis (%)				Acidity (mmol H^+ g^{-1})
	C	H	N	S	
(GO)RS-Fresh	64.93 + 0.07	1.90 + 0.02	0.11 + 0.01	5.37 + 0.01	1.676
(GO)RS-reused (5th cycle)	62.80 + 0.07	2.01 + 0.02	0.16 + 0.01	4.21 + 0.01	1.312

6. Malaika A, Kozłowski M (2019) Glycerol conversion towards valuable fuel blending compounds with the assistance of SO_3H-functionalized carbon xerogels and spheres. Fuel Process Technol 184:19–26. https://doi.org/10.1016/j.fuproc.2018.11.006
7. Calero J, Luna D, Sancho ED et al (2015) An overview on glycerol-free processes for the production of renewable liquid biofuels, applicable in diesel engines. Renew Sustain Energy Rev 42:1437–1452. https://doi.org/10.1016/j.rser.2014.11.007
8. Manurung R, Dedi Anggreawan M, Gery Siregar A (2020) Triacetin production using SiO_2-H_3PO_4 catalysts derived from bamboo leaf biomass waste for esterification reactions of glycerol and acetic acid. IOP Conf Ser Mater Sci Eng. https://doi.org/10.1088/1757-899X/801/1/012052
9. Khayoon MS, Triwahyono S, Hameed BH, Jalil AA (2014) Improved production of fuel oxygenates via glycerol acetylation with acetic acid. Chem Eng J 243:473–484. https://doi.org/10.1016/j.cej.2014.01.027
10. Testa ML, La Parola V (2021) Sulfonic acid-functionalized inorganic materials as efficient catalysts in various applications: a minireview. Catalysts. https://doi.org/10.3390/catal11101143
11. Kale S, Umbarkar SB, Dongare MK et al (2015) Selective formation of triacetin by glycerol acetylation using acidic ion-exchange resins as catalyst and toluene as an entrainer. Appl Catal A 490:10–16. https://doi.org/10.1016/j.apcata.2014.10.059
12. Cahyono RB, Mufrodi Z, Hidayat A, Budiman A (2016) Acetylation of glycerol for triacetin production using Zr-natural zeolite catalyst. ARPN J Eng Appl Sci 11:5194–5197
13. Venkatesha NJ, Bhat YS, Prakash BSJ (2016) Volume accessibility of acid sites in modified montmorillonite and triacetin selectivity in acetylation of glycerol. RSC Adv 6:45819–45828. https://doi.org/10.1039/c6ra05720a
14. Appaturi JN, Jothi Ramalingam R, Selvaraj M et al (2021) Selective synthesis of triacetyl glyceride biofuel additive via acetylation of glycerol over NiO-supported TiO_2 catalyst enhanced by non-microwave instant heating. Appl Surf Sci 545:149017. https://doi.org/10.1016/j.apsusc.2021.149017
15. Khayoon MS, Hameed BH (2011) Acetylation of glycerol to biofuel additives over sulfated activated carbon catalyst. Bioresour Technol 102:9229–9235. https://doi.org/10.1016/j.biortech.2011.07.035
16. Arbelaez Perez OF, Gonzalez Martinez CD, Salazar Henao D, Guzmán Sanchez JA (2021) Producción de acetinas (aditivos para combustibles) a partir de glicerol. Lámpsakos. https://doi.org/10.21501/21454086.3816
17. Wang L, Wang D, Zhang S, Tian H (2013) Synthesis and characterization of sulfonated graphene as a highly active solid acid catalyst for the ester-exchange reaction. Catal Sci Technol 3:1194–1197. https://doi.org/10.1039/c3cy20646g
18. Oger N, Lin YF, Labrugère C et al (2016) Practical and scalable synthesis of sulfonated graphene. Carbon N Y 96:342–350. https://doi.org/10.1016/j.carbon.2015.09.082
19. Mirza-Aghayan M, Molaee Tavana M, Boukherroub R (2016) Sulfonated reduced graphene oxide as a highly efficient catalyst for direct amidation of carboxylic acids with amines using ultrasonic irradiation. Ultrason Sonochem 29:371–379. https://doi.org/10.1016/j.ultsonch.2015.10.009
20. Ji J, Zhang G, Chen H et al (2011) Sulfonated graphene as water-tolerant solid acid catalyst. Chem Sci 2:484–487. https://doi.org/10.1039/c0sc00484g
21. Liu F, Sun J, Zhu L et al (2012) Sulfated graphene as an efficient solid catalyst for acid-catalyzed liquid reactions. J Mater Chem 22:5495–5502. https://doi.org/10.1039/c2jm16608a
22. Miranda C, Ramírez A, Sachse A et al (2019) Sulfonated graphenes: efficient solid acid catalyst for the glycerol valorization. Appl Catal A 580:167–177. https://doi.org/10.1016/j.apcata.2019.04.010
23. Marcano DC, Kosynkin DV, Berlin JM et al (2010) Improved synthesis of graphene oxide. Am Chem Soc 4:4806–4814
24. Johra FT, Lee JW, Jung WG (2014) Facile and safe graphene preparation on solution based platform. J Ind Eng Chem 20:2883–2887. https://doi.org/10.1016/j.jiec.2013.11.022
25. Pan D, Wang S, Zhao B et al (2009) Li storage properties of disordered graphene nanosheets. Chem Mater 21:3136–3142. https://doi.org/10.1021/cm900395k
26. Sahoo P, Shubhadarshinee L, Jali BR et al (2021) Synthesis and characterization of graphene oxide and graphene from coal. Mater Today Proc. https://doi.org/10.1016/j.matpr.2021.08.206
27. Stobinski L, Lesiak B, Malolepszy A et al (2014) Graphene oxide and reduced graphene oxide studied by the XRD, TEM and electron spectroscopy methods. J Electron Spectros Relat Phenomena 195:145–154. https://doi.org/10.1016/j.elspec.2014.07.003
28. Guliani D, Kaur K, Singh N et al (2019) Catalytic performance of sulfate-grafted graphene oxide for esterification of acetic acid with methanol. Chem Eng Commun 206:592–604. https://doi.org/10.1080/00986445.2018.1514601
29. Estevez R, Aguado-Deblas L, Montes V et al (2020) Sulfonated carbons from olive stones as catalysts in the microwave-assisted etherification of glycerol with tert-butyl alcohol. Mol Catal 488:110921. https://doi.org/10.1016/j.mcat.2020.110921
30. Chen Y, Zhao H, Sheng L et al (2012) Mass-production of highly-crystalline few-layer graphene sheets by arc discharge in various H_2-inert gas mixtures. Chem Phys Lett 538:72–76. https://doi.org/10.1016/j.cplett.2012.04.020
31. Ferreira P, Fonseca IM, Ramos AM et al (2011) Acetylation of glycerol over heteropolyacids supported on activated carbon. Catal Commun 12:573–576. https://doi.org/10.1016/j.catcom.2010.11.022
32. Zhou L, Nguyen TH, Adesina AA (2012) The acetylation of glycerol over amberlyst-15: kinetic and product distribution. Fuel Process Technol 104:310–318. https://doi.org/10.1016/j.fuproc.2012.06.001
33. Sandesh S, Manjunathan P, Halgeri AB, Shanbhag GV (2015) Glycerol acetins: fuel additive synthesis by acetylation and esterification of glycerol using cesium phosphotungstate catalyst. RSC Adv 5:104354–104362. https://doi.org/10.1039/c5ra17623a
34. Liao X, Zhu Y, Wang SG et al (2010) Theoretical elucidation of acetylating glycerol with acetic acid and acetic anhydride. Appl Catal B 94:64–70. https://doi.org/10.1016/j.apcatb.2009.10.021
35. Ziyang Z, Hidajat K, Ray AK (2001) Determination of adsorption and kinetic parameters for methyl tert-butyl ether synthesis from tert-butyl alcohol and methanol. J Catal 200:209–221. https://doi.org/10.1006/jcat.2001.3180
36. Ozbay N, Oktar N, Dogu G, Dogu T (2013) Activity comparison of different solid acid catalysts in etherification of glycerol with tert-butyl alcohol in flow and batch reactors. Top Catal 56:1790–1803. https://doi.org/10.1007/s11244-013-0116-0
37. Patel A, Singh S (2014) A green and sustainable approach for esterification of glycerol using 12-tungstophosphoric acid anchored to different supports: kinetics and effect of support. Fuel 118:358–364. https://doi.org/10.1016/j.fuel.2013.11.005
38. Dalla Costa BO, Decolatti HP, Legnoverde MS, Querini CA (2017) Influence of acidic properties of different solid acid catalysts for glycerol acetylation. Catal Today 289:222–230. https://doi.org/10.1016/j.cattod.2016.09.015